Chemical Science RSCPublishing

EDGE ARTICLE

Cite this: DOI: 10.1039/x0xx00000x

Received 00th January 2014,
Accepted 00th January 2014

DOI: 10.1039/x0xx00000x

www.rsc.org/

Linear Bilateral Extended 2,2′:6′,2″-Terpyridine Ligands, Their Coordination Complexes and Heterometallic Supramolecular Networks

Janis Veliks,[a] Jui-Chang Tseng,[b] Karla I. Arias,[a] Florian Weisshar,[a] Anthony Linden[a] and Jay S. Siegel*[a]

Octahedral metal complexes of tridentate 2,2′:6′,2″-terpyridine (*terpy*) fused with five-membered furan rings mimic the topology of tetrahedral metal complexes of bidentate 5,5′-functionalized 2,2′-bipyridine (*bipy*). Herein, we report the robust synthesis of 2,6-bis(2-substituted-furo[2,3-c]pyridine-5-yl)pyridine based ligands to access series of linear bilateral extended *terpy* derivatives. This molecular design of alternating five- and six-membered rings has been applied to extend the applicability of *terpy* as a building block in supramolecular chemistry. The complexation of 2,6-bis(2-substituted-furo[2,3-c]pyridine-5-yl)pyridine derivatives with metal ions preferring octahedral geometry (Fe^{2+}, Ru^{2+}, and Zn^{2+}) gives molecular "crossings" and "corners". Such design elements, functionalized with 4-pyridyl groups, allowed the construction of 3D and 2D heterometallic supramolecular networks containing Fe^{2+}, Ag^{+} or Fe^{2+}, Cu^{+} metal centers.

Introduction

De novo design and synthesis of functional supramolecular architectures benefit from ready access to components with well-defined assembly geometries.[1,2] A mainstay component[3] of supramolecular and materials chemistry, 2,2′:6′,2″-terpyridine[4] (*terpy*) ligands form coordination complexes with various metals and have photophysical and electrochemical properties suitable for supramolecular chemistry,[5] nanotechnology,[6] solar cells,[7] catalysis,[8] antitumor,[9] and antibacterial[10] research. A vast range of accessible *terpy* derivatives incorporate into geometrically well-defined supramolecular assemblies.[4,11] Examples include the synthesis of Borromean link precursors,[12] metal-organic dendrimers,[13] and molecular grids.[14]

Bifunctional molecular strings of *terpy* and *bipy* structural units, used in rotoxane-based molecular machines, switches and muscles,[15] and multi-component assemblies, such as coordination polymers,[16] and metal-organic frameworks (MOFs)[16c], reveal system properties dependant on the geometry building blocks[17] and motivate the synthesis of ligands with new geometries. Specifically, this study addresses the synthesis and characterization of *linear bilateral extended terpyridines* (Fig. 1) mimicking the linear geometry of 5,5′-functionalized 2,2′-bipyridine (*bipy* in which sites for skeletal substitution are perpendicular to the metal coordination vector).[18,19] Such ligands would allow the introduction of *terpy* into "linear" molecular assemblies – a complement to the "stub", "W", "V or Λ", and "C" motifs stemming from substituents at positions 4′, 4/4″, 5/5″, and 6/6″ with angles relative to the coordination vector of 180°, 120°, 60°, and 0°, respectively (Fig. 1A).

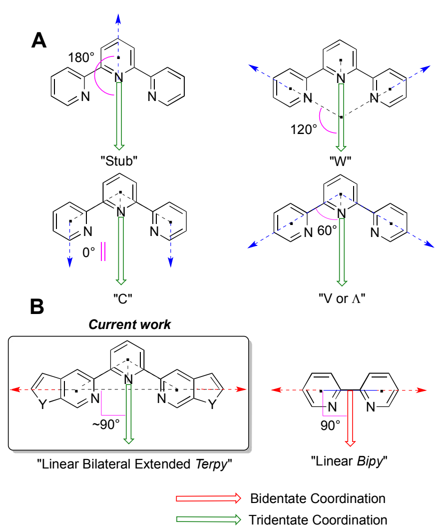

Fig. 1 A. The "Stub", "W", "V or Λ", and "C" motifs based on *terpy*. **B.** Fused five-membered rings to *terpy* mimicking 5,5′-functionalized *bipy*.

Fusion of a five-membered ring to the six-membered flanking rings of *terpy* specifically addresses the linear bilateral geometry mentioned above (Fig. 1B), and focuses this work on the practical and versatile synthesis of 2,6-bis(2-substituted-furo[2,3-c]pyridine-5-yl)pyridines (Fig. 2). Complexation of these ligands with octahedrally coordinating metal ions gives access to molecular "crossings" and "corners" suitable to the design of heterometallic supramolecular networks.

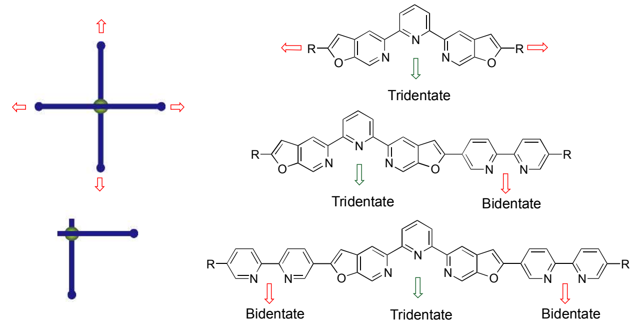

Fig. 2 Molecular design of linear bilateral extended terpyridines.

Results and discussion

Retrosynthesis

Retrosynthetic analysis of linear terpyridine **1** leads to the opening of fused five-membered rings at a heteroatom Y, giving a disubstituted ethynyl derivative **2**, which could be prepared by Sonogashira coupling[20] between dihalide **3** and acetylene **4** (Scheme 1). Terpyridine **5** stems from **6** with *ortho*-directing groups at the 5- and 5′′- positions to enable *ortho*-metalation,[21] and subsequent addition of a halide electrophile would lead to compound **3**. For Y = O, **6** is 5,5′′-hydroxy-2,2′:6′,2′′-terpyridine and the target ligands are 2,6-bis(2-substituted-furo[2,3-c]pyridine-5-yl)pyridines.

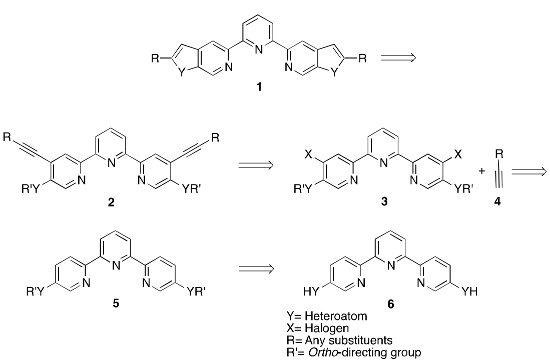

Scheme 1 Retrosynthesis of Linear Terpyridine **1**.

Synthesis of the *terpy* core

The pursuit of 2,6-bis(2-substituted-furo[2,3-c]pyridine-5-yl)-pyridine-based ligands motivated the development of an efficient chromatography-free synthesis (Scheme 2) of the key intermediate 4,4′′-diiodo-5,5′′-bis(methoxy-methoxy)-2,2′:6′,2′′-terpyridine (**14**). The route to **14** follows a Stille[22] cross-coupling strategy via **8** and **10**. Regioselective lithiation[23] of commercially available 2,5-dibromopyridine (**7**) with *n*-butyllithium and subsequent addition of 2-methoxy-4,4,5,5-tetramethyl-1,3,2-dioxaborolane gave 5-borylated pyridine **8**[24] in good yield.

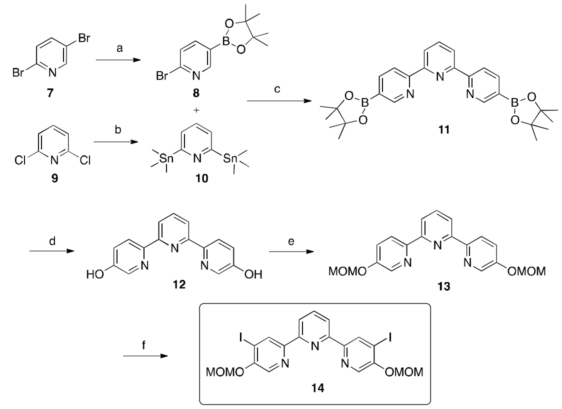

(a) *n*-BuLi, Et_2O, –78 °C, 3 h, then *B*-methoxypinacolborane, –78 °C to rt, 12 h, 83%; (b) Na, Me_3SnCl, DME, –15 °C, then **9**, –15 °C to rt, 18 h, 84%; (c) 5 mol% $Pd(PPh_3)_4$, toluene, reflux, 24 h, 56%; (d) 30% H_2O_2, aq. NaOH, THF, rt, 18 h, 96%; (e) 60% NaH, THF, DMF, 0 °C, then MOMCl/MeOAc[31], 0 °C to rt, 12 h, 96%; (f) 2.2 eq. *n*-BuLi, TMEDA, THF, –78 °C, 1 h, then 2.2 eq. I_2, –78 °C to rt, 50%.

Scheme 2 Synthesis of 4,4′′-diiodo-5,5′′-bis(methoxymethoxy)-2,2′:6′,2′′-terpyridine (**14**).

The precursor of the central ring, 2,6-bis(trimethylstannyl)pyridine (**10**), was synthesized by nucleophilic stannylation of 2,6-dichloropyridine (**9**) with freshly prepared $NaSnMe_3$ in good yield.[25,26] *Terpy* **11** was prepared by Stille coupling between bromide **8** and bisstannane **10** according to the procedure reported by Schlüter.[24] Oxidation/hydroxydeboronation[27] of **11** resulted in 5,5′′-dihydroxyterpyridine **12** in excellent yield.[28] These reactions were performed routinely on a 40 g to 90 g scale and have the potential for further scale-up. Subsequent deprotonation of hydroxy groups with NaH and treatment with MOMCl (prepared *in situ*)[29] afforded *terpy* **13**, with *ortho*-directing groups at the 5,5′′-positions. Regioselective *ortho*-lithiation[30] with *n*-BuLi in the presence of TMEDA and subsequent quenching with iodine gave the desired diiodo-*terpy* **14**. During iodine addition, a thick precipitate formed complicating both stirring and appropriate cooling. Therefore, an optimal yield was obtained when the reaction was run on a 1–3 g scale per batch. Straightforward trituration of crude product with hot ethanol afforded pure **14**.

Synthesis of acetylenes

The modular synthesis of linear bilateral *terpy* ligands requires functionalized acetylenes to incorporate desired moieties in the flanking positions. The introduction of manisyl groups[31] improves the solubility of polypyridine ligands and facilitates later homologation; therefore, several acetylenes containing this group were prepared. The synthesis of 2-ethynyl-5-methoxy-1,3-dimethylbenzene **18**[32] was accomplished according to Scheme 3. The bromide **15**[33] was converted to the iodide **16** by lithiation and subsequent quenching with iodine. Under optimized conditions for Sonogashira coupling, **16** reacted smoothly with trimethylsilylacetylene to produce silyl-protected acetylene **17**. Deprotection with KF in methanol gave **18** in high yield (Scheme 3).

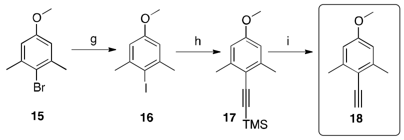

(g) *n*-BuLi, THF, –78 °C, 30 min, then I_2, –78 °C to rt, overnight, 81%; (h) trimethylsilylacetylene, 5 mol% $Pd(PPh_3)_2Cl_2$, 10 mol% CuI, toluene, Et_3N, reflux, 18 h, 95%; (i) KF, MeOH, 40 °C, 36 h, 96%.

Scheme 3 Synthesis of acetylene **18**.

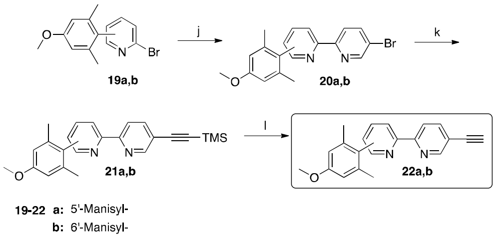

(j) 1. *n*-BuLi, THF, –78 °C, 1 h; 2. $ZnCl_2$, THF, –78 to 0 °C, 1 h; 3. **7**, 1.5 mol% $Pd(PPh_3)_4$, THF, reflux, 18 h, **20a**: 31%, **20b**: 48%[34]; (k) trimethylsilylacetylene, 10 mol% $Pd(PPh_3)_2Cl_2$, 5 mol% CuI, Et_3N, reflux, 18 h; (l) KF, MeOH, rt, 18 h, over 2 steps **22a**: 72%, **22b**: 76%.

Scheme 4 Synthesis of 5-ethynyl-2,2′-bipyridines **22**.

Manisyl substituted 5-ethynylbipyridines **22a** and **22b** were synthesized from known bromopyridines **19a**[31] and **19b**[34] (Scheme 4). Negishi coupling[35] with 2,5-dibromopyridine (**7**) afforded bromobipyridines **20a** and **20b**,[34] which coupled well with trimethylsilylacetlylene to give **21a** and **21b**. Subsequent deprotection with KF formed ethynylbipyridines **22a** and **22b** in good yields over 2 steps.

Ligand Synthesis

Simple symmetric ligand precursors – bisethynyl-*terpy* derivatives **23a, 23b**, and **23e**, as well as a mixed variation with bipyridine **23f**, were prepared by Sonogashira coupling with an excess amount (>2 eq) of corresponding alkynes in good to high yields (Table 1, entries 1, 2, 5, and 6). Due to the instability of 4-ethynylpyridine,[36] **23d** was prepared in a stepwise fashion. First, bisethynyl-*terpy* **23c** was synthesized in two steps by Sonogashira coupling between **14** and trimethylsilylacetylene following one-pot deprotection of silyl groups in the presence of KF (Table 1, entry 3). A subsequent coupling reaction with 4-iodopyridine (**25**) under standard conditions (Table 1, entry 4) gave **23d** in good yield.

To incorporate two different substituents into the 4- and 4′′-positions, Sonogashira coupling was performed with 1.05 equivalents of acetylene (Table 1, entries 7-9), giving a statistical mixture of mono- and bis-coupled products **24a-c** and **23f-h**, respectively, as well as unreacted diiodoterpyridine **14**. These mixtures were easily separated by column chromatography, and pure monosubstituted intermediates **24a-c** were obtained. The non-symmetric terpyridine/bipyridine conjugates **24a** and **24b** were further subjected to coupling with manisyl acetylene **18** to give products **26a** and **26b** in good yields (Scheme 5).

With the library of 4,4′′-disubstituted terpyridines **23a-h**, **26a** and **26b** in hand, developing general cyclization conditions to access the 2-substituted-furo[2,3-c]pyridine motif became the focus.

Table 1 Synthesis of **23** and **24** by Sonogashira coupling[a]

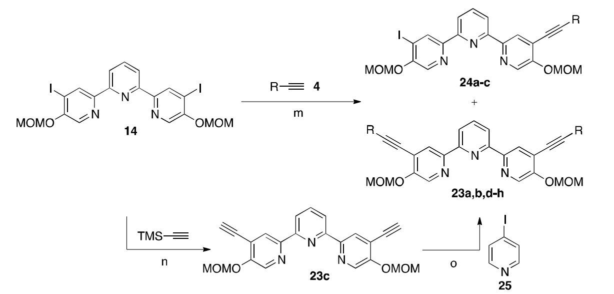

entry	R=	eq[e]	time (h)	yield (%)				
				disubst.		monosubst.		14[f]
1	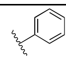	2.5	20	**23a**	95	-	-	-
2	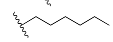	2.5	20	**23b**	92	-	-	-
3	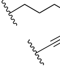	5.0	4.5[b]/18[c]	**23c**	86	-	-	-
4	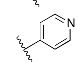	2.1[d]	20	**23d**	88	-	-	-
5	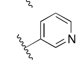	7.8	20	**23e**	85	-	-	-
6	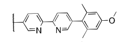	2.08	20	**23f**	90	-	-	-
7	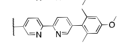	1.05	6	**23f**	18	**24a**	40	24
8	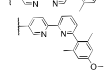	1.05	6	**23g**	17	**24b**	39	22
9	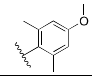	1.05	15	**23h**	15	**24c**	38	28

[a] Reaction conditions: (m) acetylene **4,** 5 mol% $Pd(PPh_3)_2Cl_2$, 10 mol% CuI, THF, Et_3N, reflux; (n) [b] trimethylsilylacetylene, 5 mol% $Pd(PPh_3)_2Cl_2$, 10 mol% CuI, THF, Et_3N, reflux, [c] then the crude mixture was subjected to TMS deprotection with KF, MeOH; (o) 1.0 eq **23c**, [d] 4-iodopyridine (**25**), 10 mol% $Pd(PPh_3)_2Cl_2$, 20 mol% CuI, THF, Et_3N, reflux. [e] Unless otherwise stated, equivalents indicated for acetylenes **4**. [f] Recovered **14**.

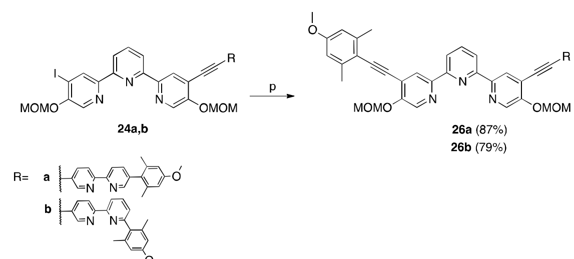

(p) Acetylene **18**, 5 mol% $Pd(PPh_3)_2Cl_2$, 10 mol% CuI, THF, Et_3N, reflux, 17-20 h.

Scheme 5 Synthesis of non-symmetric ligand precursors **26**.

In order to obtain ligand **L4**, conditions for acidic deprotection of the MOM group[37], followed by base-assisted cycloisomerization were tested on the mixed terpyridine/bipyridine **26a**. Various reaction conditions, like varying the acid, base, solvent, and reaction time, were tried (Table 2, entries 1-5). The use of HCl, Cs_2CO_3, and DMF resulted in the isolation of **L4** in high yield (Table 2, entry 5). These conditions also led to the isolation of **L1-L3**, **L5**, and **L6** (Table 2, entries 6-10) in good to high yields.

Table 2 One-pot MOM-deprotection/cycloisomerisation of **23** and **26**[a]

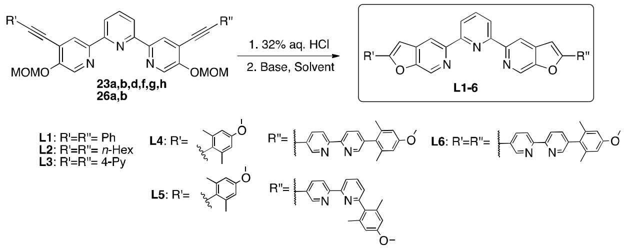

entry	SM	HCl (eq)	solvent	base	eq	time (h)	yield L	yield (%)
1[b]	**26a**	4	MeOH	NaOMe[c]	8	20	**L4**	0
2[b]	**26a**	20	MeOH	NaOMe[c]	40	40	**L4**	5
3[b]	**26a**	42	EtOH	NaOMe[c]	85	24	**L4**	11
4[b]	**26a**	42	THF	Cs_2CO_3	60	24	**L4**	19
5	**26a**	**21**	**DMF**	$\mathbf{Cs_2CO_3}$	**43**	**76**	**L4**	**97**
6	**26b**	21	DMF	Cs_2CO_3	43	48	**L5**	94
7	**23a**	5	DMF	Cs_2CO_3	43	48	**L1**	92
8	**23b**	5	DMF	Cs_2CO_3	43	48	**L2**	95
9	**23d**	5	DMF	Cs_2CO_3	43	48	**L3**	90
10	**23f**	10	DMF	Cs_2CO_3	15	72	**L6**	73

[a] 32% aq. HCl was added to the starting material (SM) in the indicated solvent and heated to 80 °C until the deprotection of MOM was complete (followed by LC-MS). Then the base was added, and the reaction mixture was heated to 90 °C for the corresponding time, unless otherwise stated. [b] Heated to reflux. [c] 5.4 M NaOMe in MeOH.

Metal complexes

A linear bilateral extended conformation of ligands can be acquired by formation of complexes with a 2:1 ligand-to-metal ratio (2:1 complexes). Initially, complexation of simple symmetric ligands **L1-L3** was tested with divalent octahedral metals (Ru^{2+}, Zn^{2+}, and Fe^{2+}) to form molecular "crossings" (Table 3). Ruthenium(II) complexes **[L1-L3₂Ru](PF₆)₂** were prepared by heating the corresponding ligands with $RuCl_2(DMSO)_4$ in ethylene glycol at 120 °C,[4c] resulting in high product yields (Table 3, entries 1, 4, and 7). Simple phenyl-substituted ligand **L1** and *n*-hexyl-substituted ligand **L2** formed 2:1 zinc(II) complexes with zinc(II) triflate in a mixture of tetrahydrofuran and methanol at room temperature (Table 3, entries 2 and 5). As 4-pyridyl-substituted ligand **L3** is less soluble, heating at 50 °C was necessary to facilitate complexation, as shown in Table 3, entry 8. Similarly, Fe^{2+} complexes were prepared by reacting iron(II) tetrafluoroborate with the corresponding ligand in a mixture of tetrahydrofuran and water at room temperature (Table 3, entries 3 and 6), but, in the case of **L3**, addition of acetonitrile to the reaction mixture was necessary to improve solubility and yield (Table 3, entry 9). All resulting metal complexes were precipitated with aqueous KPF_6 and were obtained in good to high yield.

Analogous to simple ligands **L1-L3**, mixed terpyridine/bipyridine ligands **L4-L6** reacted with $Zn(OTf)_2$ and $Fe(BF_4)_2{\cdot}6H_2O$ selectively at the terpyridine coordination site (Table 4), forming either "corner" complexes with **L4** and **L5**, or "crossing" complexes with **L6**, leaving the bipyridine coordination site unreacted. This selectivity can be explained by the kinetic lability of Zn(II) and Fe(II) complexes and the thermodynamic stability of the highest order chelate. In contrast, the kinetically inert character of Ru(II) led to a complicated mixture of oligomers when **L4-L6** were used (Table 4, entries 3, 6, and 9). Isolation of the desired 2:1 complexes was not successful. Therefore, an alternative approach towards ruthenium(II) complexes was considered for the mixed ligand systems **L4-L6**. By first introducing ruthenium(II) and then functionalizing the obtained complex with bipyridine moieties, the desired "corner" and "crossing" complexes were obtained (Scheme 6 and 7). Diiodoterpyridine **14** was subjected to complexation with 0.5 equivalents of $RuCl_2(DMSO)_4$ by heating in ethylene glycol (Scheme 6). Unexpectedly, during the reaction, the MOM protecting groups were cleaved, leading to the formation of compound **27**. This finding obviated harsh acidic conditions[37] for MOM-deprotection.

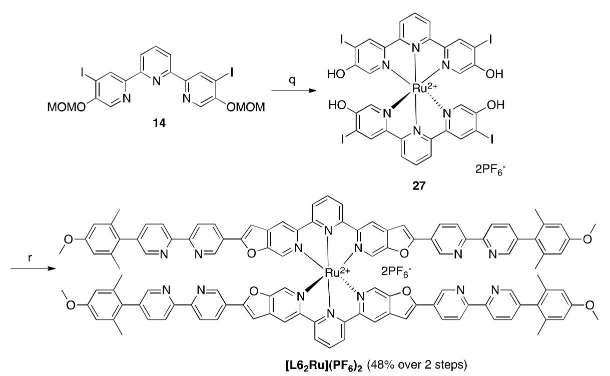

(q) 0.5 eq $RuCl_2(DMSO)_4$, ethylene glycol, 120 °C, 48 h, then aq. KPF_6; (r) 10 mol% $PdCl_2(PPh_3)_2$, 20 mol% CuI, 4.2 eq **22a**, DMF, DIPEA, 80 °C, 48 h, then aq. KPF_6.

Scheme 6 Indirect synthesis towards the ruthenium(II) complex with mixed ligand **L6**.

Crude complex **27** was used in the next step, where Sonogashira cross-coupling[20b] with acetylene **22a** and *in situ* ring closure[38] afforded compound **[L6₂Ru](PF₆)₂** directly, thus, leading to the desired complexes in just two steps starting from **14** with a 48% overall yield.

The corresponding non-symmetric Ru(II) complexes **[L4₂Ru](PF₆)₂** and **[L5₂Ru](PF₆)₂** were prepared similarly (Scheme 7). Complexation of manisyl-substituted iodoterpyridine **24c** with 0.5 eq of $Ru(DMSO)_4Cl_2$ in EtOH in one step gave complexed, deprotected, and partially cyclized product **28**, which was used without further purification in the subsequent reaction. The Sonogashira coupling with ethynylbipyridine **22a** or **22b** and one-pot cyclization gave the desired complexes with 43% or 40% isolated yields over two steps, respectively.

Table 3 Synthesis of metal complexes with simple symmetric ligands **L1-L3**[a]

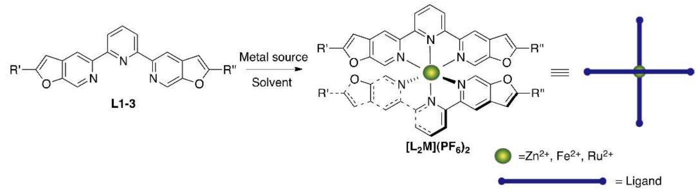

entry	ligand	R'=R''=	metal source	solvent	time (h)	T (°C)	product	Yield (%)
1	**L1**		$RuCl_2(DMSO)_4$	Ethylene glycol	18	120	**[L1₂Ru](PF₆)₂**	92
2		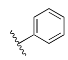	$Zn(OTf)_2$	THF/MeOH	18	rt	**[L1₂Zn](PF₆)₂**	94
3			$Fe(BF_4)_2•6H_2O$	THF/H_2O	18	rt	**[L1₂Fe](PF₆)₂**	90
4	**L2**		$RuCl_2(DMSO)_4$	Ethylene glycol	18	120	**[L2₂Ru](PF₆)₂**	99
5		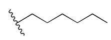	$Zn(OTf)_2$	THF/MeOH	18	rt	**[L2₂Zn](PF₆)₂**	87
6			$Fe(BF_4)_2•6H_2O$	THF/H_2O	18	rt	**[L2₂Fe](PF₆)₂**	90
7	**L3**		$RuCl_2(DMSO)_4$	Ethylene glycol	18	120	**[L3₂Ru](PF₆)₂**	98
8		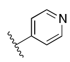	$Zn(OTf)_2$	THF/MeOH	48	50	**[L3₂Zn](PF₆)₂**	94
9			$Fe(BF_4)_2•6H_2O$	THF/MeCN/H_2O	18	rt	**[L3₂Fe](PF₆)₂**	80

[a] A solution of metal source (0.5 eq) was added to a solution of **L1-L3** (1.0 eq) and stirred at the indicated temperature. After the stated reaction time, sat. aq. KPF_6 was added to induce precipitation and the solid was collected by filtration.

Table 4 Synthesis of metal complexes with mixed terpyridine/bipyridine ligands **L4-L6**[a]

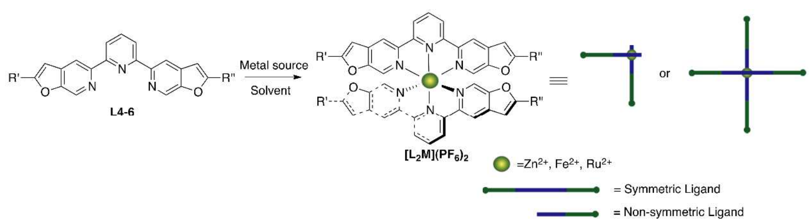

entry	ligand	R'= R''=	metal source	solvent	time (h)	T (°C)	product	Yield (%)
1	**L4**	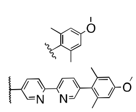	$Zn(OTf)_2$	THF/MeOH	18	rt	**[L4₂Zn](PF₆)₂**	98
2			$Fe(BF_4)_2•6H_2O$	THF/H_2O	18	rt	**[L4₂Fe](PF₆)₂**	97
3			$RuCl_2(DMSO)_4$	Ethylene glycol	48	120	**[L4₂Ru](PF₆)₂**	-[b]
4	**L5**	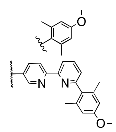	$Zn(OTf)_2$	THF/H_2O	6	rt	**[L5₂Zn](PF₆)₂**	99
5			$Fe(BF_4)_2•6H_2O$	THF/H_2O	6	rt	**[L5₂Fe](PF₆)₂**	80
6			$RuCl_2(DMSO)_4$	Ethylene glycol	48	120	**[L5₂Ru](PF₆)₂**	-[b]
7	**L6**		$Zn(OTf)_2$	THF/MeOH	20	rt	**[L6₂Zn](PF₆)₂**	92
8		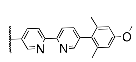	$Fe(BF_4)_2•6H_2O$	THF/H_2O	18	rt	**[L6₂Fe](PF₆)₂**	80
9			$RuCl_2(DMSO)_4$	Ethylene glycol	48	120	**[L6₂Ru](PF₆)₂**	-[b]

[a] A solution of metal source was added to a solution of **L4-L6** and stirred at the indicated temperature. After the stated reaction time, sat. aq. KPF_6 was added to induce precipitation and the solid was collected by filtration. [b] Complicated mixture, product could not be isolated.

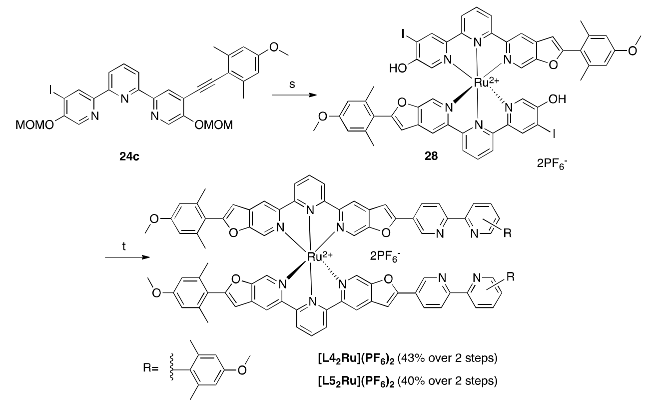

(s) 0.5 eq $RuCl_2(DMSO)_4$, EtOH, reflux, 72 h, then aq, KPF_6; (t) 5 mol% $PdCl_2(PPh_3)_2$, 10 mol% CuI, **22a** or **22b**, DMF, Et_3N, 90 °C, 24-39 h, then aq. KPF_6.

Scheme 7 Indirect synthesis towards ruthenium(II) complex with mixed ligands **L4** and **L5**.

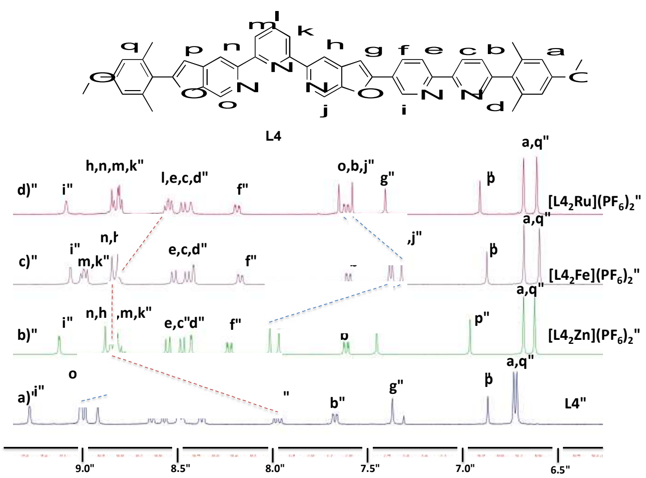

Fig. 3 ^1H NMR (400 MHz, CD_2Cl_2) for the aromatic regions in **L4** and its Zn^{2+}, Fe^{2+}, and Ru^{2+} complexes.

The ^1H NMR spectra of **[L4$_2$Zn](PF$_6$)$_2$** and **[L4$_2$Fe](PF$_6$)$_2$** (Figure 3, spectra b and c) parallel that of **[L4$_2$Ru](PF$_6$)$_2$** (spectrum d). Given that **[L4$_2$Ru](PF$_6$)$_2$** is synthesized by grafting *bipy* units on to the preformed *terpy* ruthenium(II) complex **28**, it seems reasonable to conclude that Fe(II) and Zn(II) also bind at the *terpy* unit of **L4**. Terpyridine transition metal complexes exhibit characteristic strong upfield shifts of the proton *o* and *j* signals (d-π* back-donation) and downfield shift for the signal of proton *l* (deshielding due to the conformational change of terpyiridine) compared to the shifts observed for the free ligand (Figure 3, spectrum a). The proton signals corresponding to the bipyridine moiety are less affected. These observations hold true for all Zn^{2+}, Fe^{2+}, and Ru^{2+} complexes in the ligand series **L4-L6**.

Structure

Single crystals of the free ligands **L1** and **L4** suitable for X-ray crystallography were obtained by diethyl ether vapor diffusion into a saturated dichloromethane solution. In Figure 4, the molecular structures clearly show the presence of furo[2,3-c]pyridine-5-yl motifs linked by the central 2,6-substituted pyridine ring, thus forming the desired ligand architecture. The usual conformation of uncoordinated terpyridine has a "Λ-shaped" structure with the flanking substituents placed almost perpendicular to each other, as seen for **L1** (Fig. 4a). One arm of the mixed ligand **L4** consists of furo[2,3-c]pyridine-5-yl, bipyridyl and manisyl groups in a linear disposition and the second arm is the 2-manisyl-furo[2,3-c]pyridine-5-yl unit (Fig. 4b). The manisyl rings in **L4** adopt a *clinal* conformation to the mean plane of the ligand, in contrast to the *periplanar* conformation of the simple phenyl substituents of **L1**. This deviation from planarity seen in the crystal structure of **L4**, correlates with the much better solubility of the manisyl substituted ligands **L4-L6** in common organic solvents.

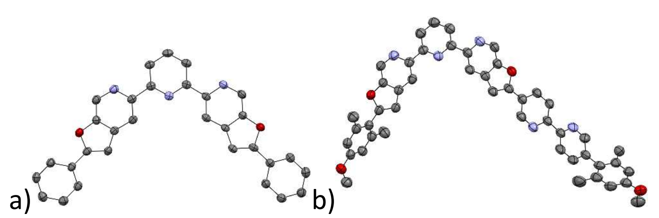

Fig. 4 The molecular structures of a) phenyl substituted ligand **L1** b) mixed bipyridine/terpyridine ligand **L4** (hydrogen atoms removed for clarity, displacement ellipsoids drawn at the 50% probability level).

The complexation of linear *terpy* ligands with metal ions preferring octahedral geometry transforms the overall ligand conformation from "Λ-shaped" to a "linear bilateral" one, as illustrated by the molecular structures of the Fe^{2+}, Ru^{2+}, and Zn^{2+} complexes with **L1** depicted in Fig. 5. Crystals for complexes **[L1$_2$Zn](PF$_6$)$_2$**, **[L1$_2$Ru](PF$_6$)$_2$**, and **[L1$_2$Fe](PF$_6$)$_2$** were obtained by diffusion of diethyl ether vapor into the corresponding acetonitrile solutions.

These crystal structures possess triclinic symmetry and belong to space group $P\bar{1}$. In each case, the asymmetric unit consists of one cation, two PF_6^- anions, and a cavity situated about a center of inversion containing disordered solvent molecules. The three structures are essentially isostructural except that the contents of the solvent cavities may differ (for the treatment and estimation of the solvent content, see the deposited CIF files in the ESI†).

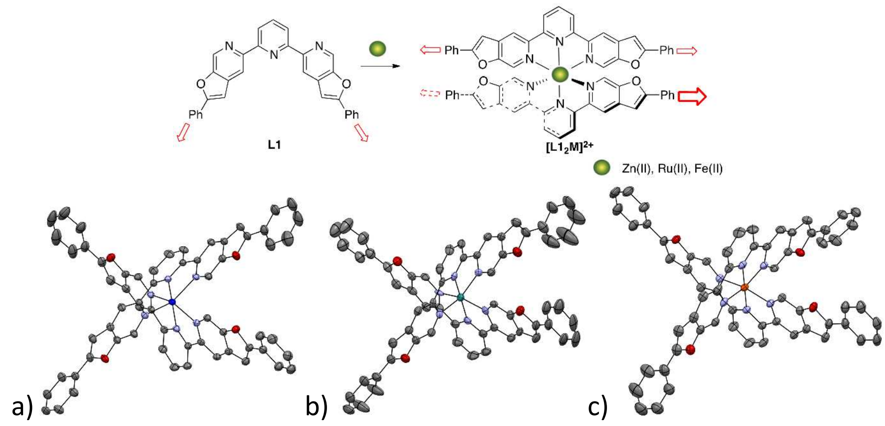

Fig. 5 The switching of **L1** conformation from "Λ-shaped" to the "linear bilateral" and the structures of the cations of a) **[L1$_2$Zn](PF$_6$)$_2$·Et$_2$O·6MeCN**; b) **[L1$_2$Ru](PF$_6$)$_2$·2Et$_2$O·3MeCN**; c) **[L1$_2$Fe](PF$_6$)$_2$·2Et$_2$O·MeCN** (hydrogen atoms, PF$_6^-$ and solvent molecules removed for clarity, displacement ellipsoids drawn at the 50% probability level).

Table 5 Selected bite angles and bond lengths of **L1** metal complexes

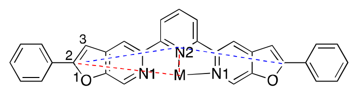

	[L1$_2$Fe](PF$_6$)$_2$	[L1$_2$Ru](PF$_6$)$_2$	[L1$_2$Zn](PF$_6$)$_2$
C(2)-N(2)-C(2) (°)[a]	142.1(3)	146.2(4)	150.1(2)
N(2)-M-C(2) (°)[b]	92.8(1)	89.9(2)	87.13(6)
M-N(1) (Å)[b]	1.971(3)	2.061(5)	2.183(2)
M-N(2) (Å)[b]	1.882(3)	1.983(4)	2.080(2)

[a] Average of two such parameters in the molecule. [b] Average of four such parameters in the molecule.

The C(2)-N(2)-C(2) bite angle in these complexes increases in the order Fe^{2+} < Ru^{2+} < Zn^{2+} (atom numbers are defined in the sketch in Table 5). For an ideally "linear" ligand topology overall, this angle should be ~160°. The ligand in the zinc complex therefore has an almost "linear" topology, while in the iron complex it has a slightly more bent character. This trend correlates with the metal-to-nitrogen bond lengths, although that is not necessarily intuitive. An increase in the M–N2 distance would tend to decrease the bite angle, whereas increases in the M–N1 distances would open it.

Photophysical properties

The UV/Vis spectra of the free ligands **L1-L6** display absorption maxima in a range of 239 to 338 nm (Fig. 6A; see ESI† Table S1). These absorptions can be attributed to π-π* transitions. The ligands **L1-L6** are fluorescent with emission maxima from 338 to 426 nm and quantum yields ranging from 0.14 to 0.62.

The absorption spectra of all zinc(II), iron(II), and ruthenium(II) complexes with **L1-L6** (Fig. 6B; see ESI† Table S2, Fig. S16, and S17) display pronounced ligand-centered (LC) transitions. However, the complexes with iron(II) and ruthenium(II) also show characteristic lower energy bands from 360 to 600 nm which can be attributed to MLCT transitions.[39] The zinc(II) complexes exhibit a fluorescence comparable to that of the parent ligands with quantum yields ranging from 0.10 to 0.63.

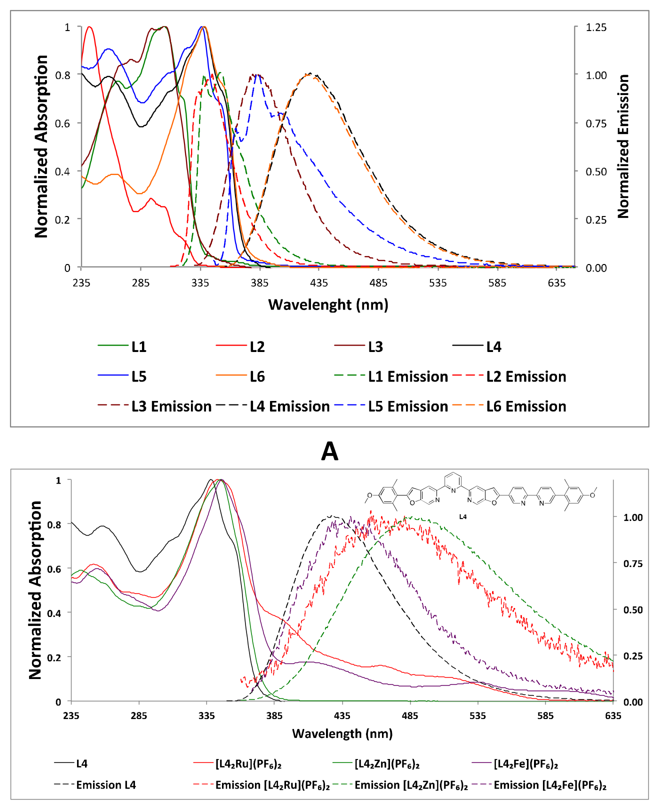

B

Fig. 6 Emission and absorption spectra of **A.** free ligands **L1-L6** and **B.** Zn(II), Fe(II) and Ru(II) complexes of **L5** in CH_2Cl_2 solution.

The MLCT bands of the iron(II) and ruthenium(II) complexes with **L1-L6** are non-luminescent at room temperature. However, excitation at the LC bands shows weak but detectable fluorescence.

The free ligands and their zinc(II) complexes exhibit solid-state emission with moderate to medium quantum yields (ESI† Tables S1 and S2). A more detailed discussion about the solution and solid-state photophysical properties of the bilateral extended *terpy* ligands **L1-L6** and their corresponding Zn(II), Fe(II), and Ru(II) complexes can be found in the Supporting Information (Table S1, S2 and Fig. S15, S16, and S17).

Heterometallic supramolecular networks

A solution of $AgPF_6$ in ethanol was layered over a solution of the 4-pyridyl substituted **$[L3_2Fe](PF_6)_2$** complex in acetonitrile. A small amount of cyclohexane between the layers was used to slow down the diffusion process. In a few days fine needle-like crystals[40] formed which over two weeks transformed into dark purple blocks that were separated by filtration to give coordination polymer **$[L3_2FeAg]_n(PF_6)_{3n}\cdot 6.5nMeCN$** (further referred to as **L3FeAg**) (Scheme 8).

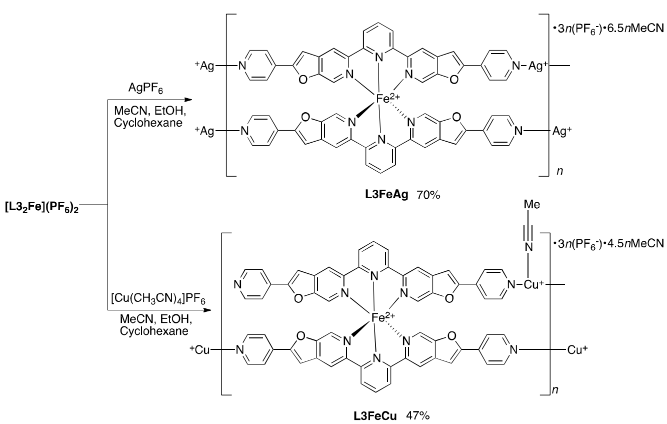

Scheme 8 Synthesis of 3D **L3FeAg** and 2D **L3FeCu** heterometallic supramolecular networks.

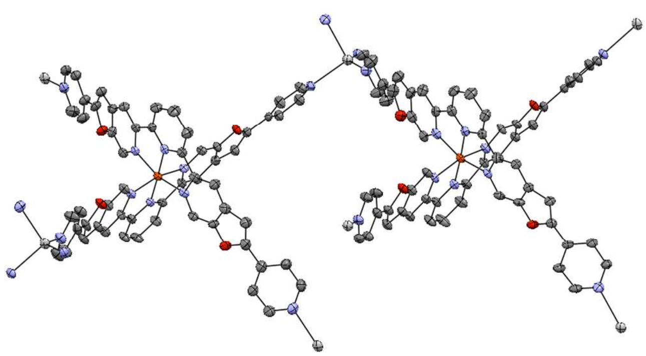

Fig. 7 The structure of the symmetry-unique part of the polymeric cation in **L3FeAg**. (Color code: Fe, orange; Ag, silver; N, light blue; O, red; C, dark gray; hydrogen atoms and PF_6^- removed for clarity, displacement ellipsoids drawn at the 50% probability level).

Similarly, a $[Cu(CH_3CN)_4]PF_6$ solution was slowly diffused into the acetonitrile solution of **$[L3_2Fe](PF_6)_2$**, using a small amount of cyclohexane between the layers. Dark purple block-like crystals were obtained over three weeks, and the resulting product **$[L3_2FeCu(MeCN)]_n(PF_6)_{3n}\cdot 4.5nMeCN$** (further referred to as **L3FeCu**) was separated by filtration (Scheme 8).

The X-ray crystal structures of complexes **L3FeAg** and **L3FeCu** revealed that they are coordination polymers. The asymmetric unit of **L3FeAg** contains two repeats of the chemically unique portion of the polymeric cation (Fig. 7), six disordered PF_6^- anions and a cavity situated about a center of inversion containing disordered solvent molecules. The cationic structure is a three-dimensional doubly interpenetrating coordination framework with (6,4) diamondoid net (**dia-b**) topology[41]. The nodes of this framework are tetrahedral silver(I) centers (Fig. 8, light blue balls) and octahedral iron(II) centers (magenta balls), where the four arms of the molecular "crossing" act as linkers. The inversion related network is interpenetrated in a manner characteristic of diamondoid type networks.[16a]

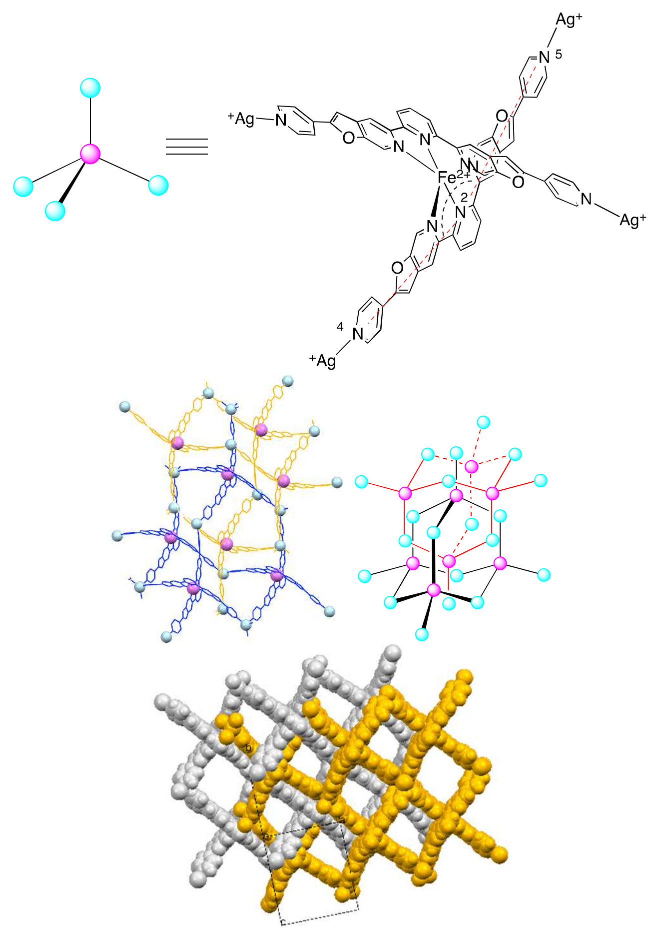

Fig. 8 The diamondoid net (**dia-b**) topology of **L3FeAg** and interpenetration.

The structure of the iron(II) based molecular "crossings" reveal that the furo[2,3-*c*]pyridine arms of the ligand are significantly tilted; therefore, the angle between the N atoms of both flanking 4-pyridiyl groups and the N atom of the central ring of *terpy*, N(4)-N(2)-N(5), is 134.43(5)°. The shortest Ag(1)···Ag(2) and Fe(1)···Fe(2) distances within a single net are 16.9095(6) and 16.7399(8) Å, respectively. This causes significant voids and channels within the structure. Each unit cell contains one solvent-filled centrosymmetric cavity which comprises 31.5% of the total volume (calculated using PLATON[42]).

The X-ray crystal structure of **L3FeCu** shows that Fe(II) based molecular "crossings" in the presence of Cu(I) assemble into a structure similar to that of **L3FeAg**. However, one coordination site of the tetrahedral Cu(I) center is occupied by acetonitrile (Fig. 9). Consequently, one of four 4-pyridyl groups, which is disordered, is not coordinated to the copper atom and the cationic structure of **L3FeCu** consists of stacked 2D polymeric layers with a (6,3) honycomb (**hcb**)[41] net topology (Fig. 10). Adjacent layers are related by inversion symmetry. The nodes of this framework are tetrahedral copper(I) centers (Fig. 10, dark red balls) and octahedral iron(II) centers (magenta balls), where only three arms of the molecular "crossing" act as linkers.

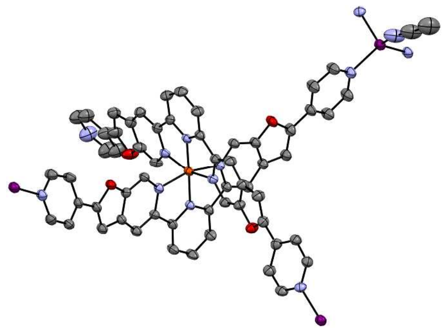

Fig. 9 The structure of the symmetry-unique part of the polymeric cation in **L3FeCu**. (Color code: Fe, orange; Cu, purple; N, light blue; O, red; C, dark gray; hydrogen atoms and PF_6^- removed for clarity, displacement ellipsoids drawn at the 50% probability level).

The shortest Fe(1)···Fe(1) and Cu(1)···Cu(1) distances within each net are 16.7466(6) and 18.3235(6) Å, respectively. The angle between the N atoms of flanking 4-pyridiyl groups at the N atom of the central ring of *terpy*, N(10)-N(7)-N(9), is 135.23(5)°.

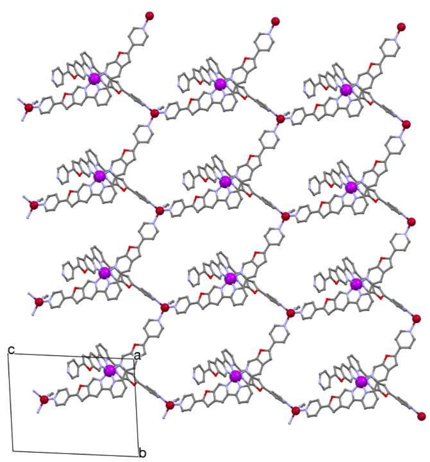

Fig. 10 Ball and stick representation of one cationic layer of **L3FeCu** viewed down the *a* axis. (Color code: Fe, magenta; Cu, dark red; N, light blue; O, red; C, dark gray).

While the **L3FeAg** and **L3FeCu** structures are similar (Fig. 11), the 3D topology in **L3FeAg** is reduced to a 2D layer network by replacing a pyridine connection to silver with a competing MeCN ligand in **L3FeCu**. Interestingly, in **L3FeAg**, the Ag–N(pyridyl) bond lengths at each unique Ag(I) cation are grouped into two pairs of distinctly different distances, one with an average distance of 2.25 Å and the other pair at 2.41 Å.

The ^{1}H and ^{13}C NMR spectra of vacuum dried and dissolved crystals of **L3FeAg** and **L3FeCu** in acetonitrile-d_3 are almost identical to that of $\mathbf{[L3_2Fe](PF_6)_2}$ suggesting that the solid state structure disassociates in solution. The proton signals of the 4-pyridyl groups are slightly shifted due to the presence of Ag^+ or Cu^{2+} ions.

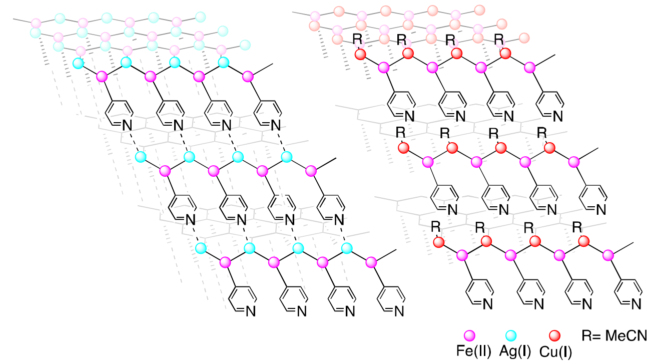

Fig. 11 Schematic representation of the 3D cationic structure of **L3FeAg** and 2D layered cationic structure of **L3FeCu**.

Conclusions

The concept of a linear bilateral extended terpyridine was developed by fusing five-membered rings to the flanking pyridine rings of the *terpy* ligand, thus mimicking the extended geometry of 5,5′-functionalized 2,2′-bipyridine. It was realized synthetically by developing a modular synthesis of 2,6-bis(2-substituted-furo[2,3-c]pyridine-5-yl)pyridine based ligands. This modular synthesis allowed for the introduction of alkyl, aryl, and heteroaryl functionalities in the flanking positions of these ligands. The molecular "crossings" were synthesized by coordinating simple symmetric ligands to divalent metal cations (Fe^{2+}, $Ru^{2+}$and Zn^{2+}) forming 2:1 complexes. In the case of mixed bipyridine/terpyridine ligands, zinc(II) and iron(II) selectively form complexes at the terpyridine coordination site. The corresponding ruthenium(II) complexes were prepared through an indirect methodology. First, unfunctionalized ruthenium(II) terpyridine 2:1 complexes were prepared, then bipyridyl groups were introduced through a one-pot Sonogashira coupling with an *in situ* furan ring formation. In this way, the *terpy* and *bipy* moieties arrange themselves in a linear rod motif. These complexes resemble molecular "crossings" and "corners", depending on whether symmetric or non-symmetric starting materials were used in the reaction. The X-ray crystal structures of symmetric phenyl substituted analogues showed that a proper "linear bilateral" conformation of *terpy* ligands is acquired by complexation with metal ions, so that flanking substituents are spanned relative to each other with an obtuse angle. This angle increases in the sequence of $Fe^{2+}<Ru^{2+}<Zn^{2+}$. The free ligands show high to medium fluorescence quantum yields that are significantly quenched by complexation with Fe^{2+} and Ru^{2+} ions. The zinc(II) complexes still retain a fluorescence efficiency similar to that of their parent ligands. The free ligands and their zinc(II) complexes exhibit solid-state emission with moderate to medium quantum yields, so could find an application as optoelectronic materials. This molecular design has potential in supramolecular chemistry giving new topological features to terpyridine, which now mimics the linear geometry of 5,5′-disubstituted 2,2′-bipyridine. It has been shown that linear bilateral extended *terpy* based Fe(II) "crossings" functionalized with 4-pyridiyl groups at the flanking positions are able to assemble into 3D and 2D heterometallic supramolecular networks by using Ag(I) or Cu(I), respectively. Substitution of the flanking positions of linear bilateral extended *terpy* with directionally functional

groups allows the construction of supramolecular assemblies and extended networks. Given the fact that a convenient synthesis of these ligands has been developed, various functional groups can easily be introduced to address other supramolecular interactions like hydrogen or donor-acceptor bonding, as well as strong metal-carboxylate bonds, which are used extensively in the field of MOFs.

Therefore, linear bilateral extended *terpy* based fundamental building blocks with "crossing" and "corner" character are new tools in the hands of chemists and could inspire the creation of new designed molecular architectures.

Acknowledgements

This work was funded by Swiss National Science Foundation. We thank PD Dr. Laurent Bigler and Urs Stadler for measuring mass spectra, Peter Uebelhart for his work on X-ray crystal structures.

Notes and references

[a] Department of Chemistry, University of Zurich, Winterthurerstrasse 190, 8057 Zurich, Switzerland. E-mail: jss@oci.uzh.ch
[b] Chaoyang University of Technology, Department of Applied Chemistry, 168, Jifeng E. Rd., Wufeng District, Taichung, 41349 Taiwan, R.O.C.
† Electronic Supplementary Information (ESI) available: Full experimental synthesis procedures and characterization data, including ^{1}H NMR and ^{13}C NMR spectra of all new compounds and CIF files. See DOI: 10.1039/b000000x/

1 (a) P. J. Stang, *Chem. Eur. J.*, 1998, **4**, 19; (b) S. Leininger, B. Olenyuk and P. J. Stang, *Chem. Rev.*, 2000, **100**, 853; (c) R. Chakrabarty, P. S. Mukherjee and P. J. Stang, *Chem. Rev.*, 2011, **111**, 6810.
2 (a) M. Fujita, Y. J. Kwon, S. Washizu and K. Ogura, *J. Am. Chem. Soc.*, 1994, **116**, 1151; (b) D. L. Caulder, C. Brückner, R. E. Powers, S. König, T. N. Parac, J. A. Leary and K. N. Raymond, *J. Am. Chem. Soc.*, 2001, **123**, 8923; (c) M. Fujita, Y. J. Kwon, S. Washizu and K. Ogura, *Acc. Chem. Res.*, 2005, **38**, 371.
3 (a) J.-M. Lehn, *Angew. Chem. Int. Ed. Engl.*, 1988, **27**, 89; (b) F. Vögtle, *Supramolecular Chemistry*, Wiley, Chichester, 1991; (c) J.-M. Lehn, *Supramolecular Chemistry-Concepts and Perspectives*, VHC, Weinheim, 1995; (d) M. M. Safont-Sempere, G. Fernàndez and F. Würthner, *Chem. Rev.*, 2011, **111**, 5784.
4 (a) S. G. Morgan and F. H. Burstall, *J. Chem. Soc.*, 1931, 20; (b) S. G. Morgan and F. H. Burstall, *J. Chem. Soc.*, 1937, 1649–1655; (c) E. C. Constable and M. W. C. Thompson, *New J. Chem.*, 1992, **16**, 855; (d) H. Hofmeier and U. S. Schubert, *Chem. Soc. Rev.*, 2004, **33**, 373; (e) U. S. Schubert, H. Hofmeier and G. R. Newkome, *Modern Terpyridine Chemistry*, Wiley-VCH, Weinheim, 2006.
5 (a) J.-P. Sauvage and M. Ward, *Inorg. Chem.*, 1991, **30**, 3869; (b) M. Benaglia, F. Ponzini, C. R. Woods and J. S. Siegel, *Org. Lett.*, 2001, **3**, 967; (c) E. C. Constable, *Chem. Soc. Rev.*, 2007, **36**, 246; (d) E. Coronado, J. R. Galan-Mascaros, P. Gaviña, C. Mart-Gastal-do, F. M. Romero and S. Tatay, *Inorg. Chem.*, 2008, **47**, 5197.
6 (a) T. B. Norsten, B. L. Frankamp and V. M. Rotello, *Nano Lett.*, 2002, **12**, 1345; (b) T.-Y. Dong, C.-L. Hunag, C.-P. Chen and M.-C. Lin, *J. Organomet. Chem.*, 2007, **692**, 5147; (c) A. Winter, M. D. Hager, G. R. Newkome and U. S. Schubert, *Adv. Mater.*, 2011, **23**, 5728.
7 (a) B. O'Regan and M. Grätzel, *Nature*, 1991, **353**, 737; (b) S. Ardo and G. J. Meyer, *Chem. Soc. Rev.*, 2009, **38**, 115.
8 A. Winter, G. R. Newkome and U. S. Schubert, *ChemCatChem*, 2011, **3**, 1384.
9 (a) G. Lowe, A. S. Droz, J. J. Park and G. W. Weaver, *Bioorg. Chem.*, 1999, **27**, 477; (b) K. Becker, C. Herold-Mende, J. J. Park, G. Lowe and R. H. Schirmer, *J. Med. Chem.*, 2001, **44**, 2784; (c) M. Dobroschke, Y. Geldmacher, I. Ott, M. Harlos, L. Kater, L. Wagner, R. Gust, W. S. Sheldrick and A. Prokop, *ChemMedChem,* 2009, **4**, 177; (d) B.-S. Jeong, H. Choi, Y.-S. Kwak and E.-S. Lee, *Bull. Korean Chem. Soc.*, 2011, **32**, 3566.
10 (a) A. Jain, B. S. J. Winkel and K. J. Brewer, *J. Inorg. Biochem.*, 2007, **101**, 1525; (b) A. Anthonysamy, S. Balasubramanian, V. Shanmugaiah and N. Mathivanan, *Dalton Trans.*, 2008, 2136.
11 (a) R.-A. Fallahpour, *Synthesis*, 2003, 155; (b) M. Heller and U. S. Schubert, *Eur. J. Org. Chem.*, 2003, 947; (c) P. Gaviña and S. Tatay, 2006, **47**, 3471.
12 J. C. Loren, M. Yoshizawa, R. F. Haldimann, A. Linden and J. S. Siegel, *Angew. Chem. Int. Ed.*, 1998, **37**, 2364.
13 E. C. Constable, *Chem. Commun.*, 1997, 1073.
14 D. M. Bassani, J.-M. Lehn, K. Fromm and D. Fenske, *Angew. Chem. Int. Ed.*, 1998, **37**, 2364.
15 (a) N. Armaroli, V. Balzani, J.-P. Collin, P. Gaviña, J.-P. Sauvage and B. Ventura, *J. Am. Chem. Soc.*, 1999, **121**, 4397; (b) J.-P. Collin, C. Dietrich-Buchecker, P. Gaviña, M. C. Jimenez-Molero and J.-P. Sauvage, *Acc. Chem. Res.*, 2001, **34**, 477; (c) S. Durot, F. Reviriego and J.-P. Sauvage, *Dalton Trans.*, 2010, **39**, 10557–10570.
16 (a) B. F. Hoskins and R. Robson, *J. Am. Chem. Soc.*, 1990, **112**, 1546; (b) I. Manners, *Synthetic Metal-Containing Polymers*, Wiley-VCH, 2004; (c) O. M. Yaghi, H. Li, M. Eddaoudi and M. O'Keeffe, *Nature*, 1999, **402**, 276; (d) H. Furukawa, K. E. Cordova, M. O'Keeffe and O. M. Yaghi, *Science*, 2013, **341**, 1230444.
17 (a) R. B. Getman, Y. S. Bae, C. E. Wilmer and R. Q. Snurr, *Chem. Rev.*, 2012, **112**, 703; (b) J. R. Li, J. Sculley and H. C. Zhou, *Chem. Rev.*, 2012, **112**, 869; (c) S. Yang, J. Sun, A. J. Ramirez-Cuesta, S. K. Callear, W. I. David, D. P. Anderson, R. Newby, A. J. Blake, J. E. Parker, C. C. Tang and M. Schroder, *Nat. Chem.*, 2012, **4**, 887; (d) Q. Li, W. Zhang, O. S. Miljanic, C. H. Sue, Y. L. Zhao, L. Liu, C. B. Knobler, J. F. Stoddart and O. M. Yaghi, *Science*, 2009, **325**, 855.
18 For the first synthesis of 2,2′-bipyridine and reviews, see: (a) F. Blau, *Monatsh. Chem.*, 1889, **10**, 375; (b) C. Kaes, A. Katz and M. W. Hosseini, *Chem. Rev.*, 2000, **100**, 3553; (c) V. Balzani, G. Bergamini, F. Marchioni and P. Ceroni, *Coord. Chem. Rev.*, 2006, **250**, 1254. For the examples of 5,5′-functionalized 2,2′-bipyridines, see: (d) A. Khatyr and R. Ziessel, *J. Org. Chem.*, 2000, **65**, 7814; (e) C. J. Matthews, M. R. J. Elsegood, G. Bernardinelli, W. Clegg and A. F. Williams, *Dalton Trans.*, 2004, 492.
19 The term "linear bilateral extended 2,2′:6′,2″-terpyridine" was chosen to describe *terpy* based scaffold represented in Fig. 1B, because it mimics the linear or extended geometry of 5,5′-disubstituted 2,2′-bipyridine and has "two-sided" or *bilateral* character. For definition of "bilateral," see: *The Oxford English Dictionary. 7th ed.* OUP, Oxford, 2005.

20 (a) K. Sonogashira, Y. Tohda and N. Hagihara, *Tetrahedron Lett.*, 1975, **50**, 4467. (b) Recent example of Sonogashira coupling performed directly on the Ru(II) bis-*terpy* complexes: J. Yang, J. K. Clegg, Q. Jiang, X. Lui, H. Yan, W. Zhong and J. E. Beves, *Dalton Trans.*, 2013, **42**, 15625.
21 (a) H. Gilman and R. L. Bebb, *J. Am. Chem. Soc.*, 1939, **61**, 109; (b) G. Wittig and G. Fuhrman, *Chem. Ber.*, 1940, **73**, 1197; (c) V. Snieckus, *Chem. Rev.*, 1990, **90**, 879.
22 J. K. Stille, *Angew. Chem. Int. Ed. Engl.*, 1986, **25**, 508.
23 W. E. Parham and R. M. Piccirilli, *J. Org. Chem.*, 1977, **42**, 257.
24 U. Lehmann, O. Henze and A. D. Schlüter, *Chem. Eur. J.*, 1999, **5**, 854.
25 U. S. Schubert and C. Eschbaumer, *Org. Lett.*, 1999, **1**, 1027.
26 (a) Y. Yamamoto and A. Yanagi, *Chem. Pharm. Bull.*, 1982, **30**, 1731; (b) G. F. Silbestri, M. J. Lo Fiego, M. T. Lockhart and A. B. Chopa, *J. Organomet. Chem.*, 2010, **695**, 2578.
27 A. S. Voisin, A. Bouillon, J.-C. Lancelot and S. Rault, *Tetrahedron*, 2005, **61**, 1417.
28 N. Belfrekh, C. Dietrich-Buchecker and J.-P. Sauvage, *Inorg. Chem.*, 2000, **39**, 5169.
29 M. A. Berliner and K. Belecki, *J. Org. Chem.*, 2005, **70**, 9618.
30 (a) M. R. Winkle and R. C. Ronald, *J. Org. Chem.*, 1982, **47**, 2101; (b) F. Le Strat, D. C. Harroween and J. Maddaluno, *J. Org. Chem.*, 2005, **70**, 489; (c) R. Azzouz, L. Bischo☐, C. Fruit and F. Marsais, *Synlett*, 2006, 1908
31 Manisole = 3,5-dimethylanisole; manisyl = 4-methoxy-2,6-dimethylphenyl. J. C. Loren and J. S. Siegel, *Angew. Chem. Int. Ed.*, 2001, **40**, 754.
32 (a) K. Yates and G. Mandrapilias, *J. Org . Chem.*, 1980, **45**, 3902; (b) Z. Shijun, C. Jensen, L. Sheng, M. Amane and C. Hyunsik, W.O. Patent 2,010,141,758, Dec 9, 2010.
33 (a) F. C. Goerth, M. Rucker, M. Eckhardt and R. Brueckner, *Eur. J. Org. Chem.*, 2000, **14**, 2605; (b) E. Zysman-Colman, K. Arias and J. S. Siegel, *Can. J. Chem.*, 2009, **87**, 440.
34 K. I. Arias, E. Zysman-Colman, J. C. Loren, A. Linden and J. S. Siegel, *Chem. Commun.*, 2011, **47**, 9588.
35 (a) E. Negishi, *J. Org. Chem.*, 1977, **42**, 1821; (b) E. Negishi and T. Takahashi, *Org. Synth.*, 1988, **66**, 67.
36 S. Rubinsztajn, W. K. Fife and M. Zeldin, *Tetrahedron Lett.*, 1992, **33**, 1821.
37 (a) J. Auerback and S. M. Weinreb, *J. Chem. Soc., Chem. Commun.*, 1974, 298; (b) A. I. Meyers, J. L. Durandetta and R. Munavu, *J. Org. Chem.*, 1975, **40**, 2025.
38 (a) A. C. Arcadi, S.; Marinelli, F., *Synthesis*, 1986, 749; (b) N. G. Kundu, M. Pal, J. S. Mahanty and M. De, *J. Chem. Soc., Perkin Trans. 1*, 1997, 2815; (c) A. Arcadi, S. Cacchi, S. Di Giuseppe, G. Fabrizi and F. Marinelli, *Synlett*, 2002, **3**, 453.
39 K. Kalyanasundaram, *Photochemistry of Polypyridine and Porphyrin Complexes*, Academic Press, London, 1992.
40 The initially formed needles were too small to perform single crystal X-ray analysis. Attempts at XRD analysis either as free powder or as solvated needles in capillary yielded ambiguous results. The question of whether this morphological transformation is connected to an internal structural change or a kinetic crystal growth issue remains open; however, the observation is reproducible and the final state consistently the blocks reported as **L3FeAg**.
41 (a) Reticular Chemistry Structure Resource, http://rcsr.anu.edu.au/nets/dia-b ; (b) M. O'Keeffe and O. M. Yaghi, *Chem. Rev.*, 2012, **112**, 675; (c) S. R. Batten, S. M. Neville and D. R. Turner, *Coordination Polymers: Design, Analysis and Application*, Royal Society of Chemistry, 2008.
42 A. L. Spek, *Acta Crystallogr. Sect. D*, 2009, **65**, 148.